Search for Neutrino CP Violation in the 3 Flavor Paradigm

Mary Bishai

Brookhaven National Laboratory, P.O. Box 5000, Upton, NY 11973

June 25, 2013

1 Introduction

In the 3 flavor mixing model, the PMNS matrix can be parameterized as the product of three 2-flavor mixing matrices as follows:

$$U_{PMNS} = \underbrace{\begin{pmatrix} 1 & 0 & 0 \\ 0 & c_{23} & s_{23} \\ 0 & -s_{23} & c_{23} \end{pmatrix}}_{\text{I}} \underbrace{\begin{pmatrix} c_{13} & 0 & e^{i\delta_{\text{CP}}} s_{13} \\ 0 & 1 & 0 \\ -e^{i\delta_{\text{CP}}} s_{13} & 0 & c_{13} \end{pmatrix}}_{\text{II}} \underbrace{\begin{pmatrix} c_{12} & s_{12} & 0 \\ -s_{12} & c_{12} & 0 \\ 0 & 0 & 1 \end{pmatrix}}_{\text{III}} \tag{1}$$

where $c_{\alpha\beta} = \cos\theta_{\alpha\beta}$ and $s_{\alpha\beta} = \sin\theta_{\alpha\beta}$

The "interference" term, II which describes the mixing between the 1 and 3 mass states contains the CP violating phase δ_{cp}. Leptonic CP violation in the 3 flavor model is a function of all three mixing angles and the CP phase as described by the Jarlskog invariant [1]:

$$J_{CP}^{PMNS} \equiv \frac{1}{8} \sin 2\theta_{12} \sin 2\theta_{13} \sin 2\theta_{23} \cos\theta_{13} \sin\delta_{cp} \tag{2}$$

Given the current best fit values of the mixing angles [2] and assuming a normal hierarchy, we find

$$J_{CP}^{PMNS} = 0.035 \sin\delta_{cp} \tag{3}$$

The large values of the mixing angles in the lepton sector imply that there can potentially be very large leptonic CP violation - depending on the value of the unknown phase δ_{cp} - whereas the very small mixing in the quark sector leads to very small value of the equivilant Jarlskog invariant [6] of

$$J_{CP}^{CKM} \approx 3 \pm 1 \times 10^{-5} \tag{4}$$

In the 3 flavor model, if CPT invariance is assumed then $P(\nu_l \to \nu_l) = P(\bar{\nu}_l \to \bar{\nu}_l)$ [3] which is consistent with the precision measurements from the MINOS experiment of $\nu_\mu \to \nu_\mu$, $l = e, \mu, \tau$ and $\bar{\nu}_\mu \to \bar{\nu}_\mu$ oscillations [4]. This implies that experimentally CP violation can only be accessed using appearance experiments. To probe CP violation in neutrinos, appearance experiments probing the oscillations between $\nu_{\mu,e} \to \nu_{e,\mu}$ are the most accessible experimentally. The oscillation probability of $\nu_{\mu,e} \to \nu_{e,\mu}$ through matter in a constant density approximation and keeping terms up to second order in $|\alpha| \equiv |\Delta m_{21}^2|/|\Delta m_{31}^2|$ and $\sin^2\theta_{13}$ is [5, 3]

$$P(\nu_\mu \to \nu_e) \cong P(\nu_e \to \nu_\mu) \cong P_0 + \underbrace{P_{\sin\delta}}_{\text{CP violating}} + P_{\cos\delta} + P_3 \tag{5}$$

where

$$P_0 = \sin^2\theta_{23} \frac{\sin^2 2\theta_{13}}{(A-1)^2} \sin^2[(A-1)\Delta] \tag{6}$$

$$P_3 = \alpha^2 \cos^2\theta_{23} \frac{\sin^2 2\theta_{12}}{A^2} \sin^2(A\Delta) \tag{7}$$

$$P_{\sin\delta} = \alpha \frac{8 J_{cp}}{A(1-A)} \sin\Delta \sin(A\Delta) \sin[(1-A)\Delta] \tag{8}$$

$$P_{\cos\delta} = \alpha \frac{8 J_{cp} \cot\delta}{A(1-A)} \cos\Delta \sin(A\Delta) \sin[(1-A)\Delta] \tag{9}$$

where
$$\alpha = \Delta m_{21}^2/\Delta m_{31}^2, \ \Delta = \Delta m_{31}^2 L/4E, \ \ A = \sqrt{3}G_F N_e 2E/\Delta m_{31}^2$$

CP violation can thus be probed using oscillations of muon neutrinos from accelerator neutrino beams produced from pion decays in flight and at rest, oscillations of electron neutrinos produced from muon storage rings in neutrino factories, and oscillations of atmospheric muon neutrinos. As shown in equation 1, the CP phase appears in the PMNS matrix through the mixing of the 1-3 states, therefore the physical characteristics of the appearance experiment are determined by the baseline and neutrino energy at which the mixing between the 1-3 state is maximal as follows:

$$\frac{L(\text{km})}{E_\nu(\text{GeV})} \ = \ (2n-1)\frac{\pi}{2}\frac{1}{1.27 \times \Delta m_{31}^2(\text{eV}^2)} \tag{10}$$
$$\approx \ (2n-1) \times 510\text{km/GeV} \tag{11}$$

where $n = 1, 2, 3...$ denotes the oscillation nodes at which the appearance probability is maximal. Equation 11 is for vacuum oscillations, matter effects will distort the scale at which the mixing between the 1 and 3 states is maximal. In Figures ??, the oscillation probabilities given in Equations 5 to 9 for $\nu_\mu \to \nu_e$ as a function of baseline in km and energy in GeV are shown in the oscillograms for $\delta_{cp} = 0$. The oscillograms include the matter effect assuming a constant density of the earths mantle of 2.8 g/cm^3. The solid black curves on the oscillograms indicate the location of the first and second oscillation maximum as given by equation 11. The projection of the oscillation probability versus E_ν at $L = 1300$ km is shown on the right. The different colored curves demonstrate the variation in the ν_e appearance probability as a function of the value of δ_{cp}. The variation in the $\nu_\mu \to \nu_e$ oscillation probabilities with the value of δ_{cp} indicates that it is experimentally possible to measure the value of δ_{cp} at a fixed baseline using only the observed shape of the $\nu_\mu \to \nu_e$ OR $\bar\nu_\mu \to \bar\nu_e$ appearance signal measured over an energy range that encompasses at least one full oscillation interval. A measurement of the value of $\delta_{cp} \neq 0$ or π implies that CP is violated if neutrino mixing follows the 3 flavor model, nevertheless evidence for CP violation in the neutrino sector requires the explicit observation of an asymmetry between $P(\nu_l \to \nu_{l'})$ and $P(\bar\nu_l \to \bar\nu_{l'})$. The CP asymmetry, $\mathcal{A}_{cp}$ is defined as

$$\mathcal{A}_{cp} = \frac{P(\nu_\mu \to \nu_e) - P(\bar\nu_\mu \to \bar\nu_e)}{P(\nu_\mu \to \nu_e) + P(\bar\nu_\mu \to \bar\nu_e)} \tag{12}$$

In the 3 flavor model the asymmetry can be approximated to leading order in Δm_{21}^2 as [6]:

$$\mathcal{A}_{cp} \sim \frac{\cos\theta_{23}\sin 2\theta_{12}\sin\delta}{\sin\theta_{23}\sin\theta_{13}}\left(\frac{\Delta m_{21}^2 L}{4E_\nu}\right) + \text{matter effects} \tag{13}$$

It is important to note that for $\nu_{\mu,e} \to \nu_{e,\mu}$ oscillations that proceed as the neutrinos propagate through matter, the scattering of ν_e off of electrons in matter introduces a coherent forward scattering amplitude that adds an extra interference term to the vacuum oscillations. This is the Mikheyev-Smirnov-Wolfenstein (MSW) effect [7]. The MSW effect has been observed in solar oscillation experiments [8, 9]. The matter effect depends on the mass hierarchy as shown in the oscillograms in Figures ?? as follows:

- For normal hierarchy $P(\nu_\mu \to \nu_e)$ is enhanced and $P(\bar\nu_\mu \to \bar\nu_e)$ is suppressed. The effect increases with baseline at a fixed L/E.

- For inverted hierarchy $P(\nu_\mu \to \nu_e)$ is suppressed and $P(\bar\nu_\mu \to \bar\nu_e)$ is enhanced. The effect increases with baseline at a fixed L/E.

- The matter effect has the largest impact on the probability amplitude at the 1st oscillation maxima.

- The matter effect introduces a phase shift in the oscillation pattern. The oscillation pattern is shifted to a lower energy for a given baseline when the hierarchy changes from normal to inverted. The shift is ≈ -100 MeV.

In Figure 3, the asymmetries induced by matter and maximal CP violation (at $\delta_{cp} = \pm pi/2$) are shown separately as a 2-D oscillograms in baseline and neutrino energy. The impact of the matter effect is therefore to introduce a matter induced asymmetry in $P(\nu_l \to \nu_{l'})$ and $P(\bar\nu_l \to \bar\nu_{l'})$ that is in addition to the CP asymmetry - if any - induced through the CP violating phase, δ_{cp}. At longer baselines ($> 1000km$), the matter asymmetry in the energy region of the first oscillation node is driven primarily by the change in the ν_e appearance amplitude. At shorter baselines ((100) km) the asymmetry is driven by the phase shift. In general:

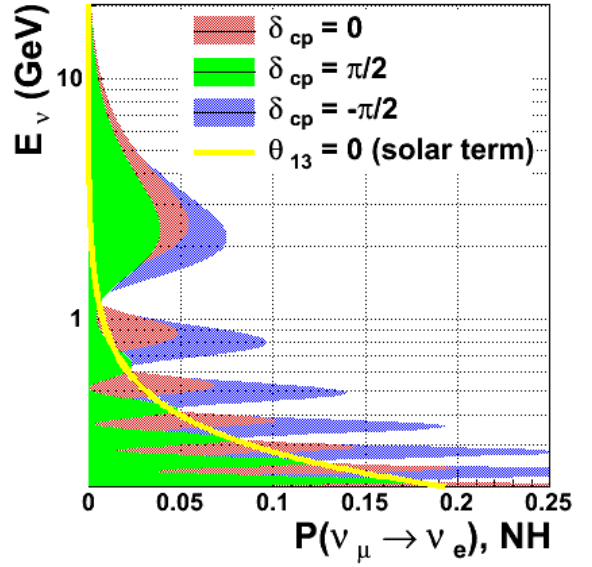$$\mathcal{A}_{cp} \ \propto \ L/E \tag{14}$$
$$\mathcal{A}_{matter} \ \propto \ L \times E \tag{15}$$
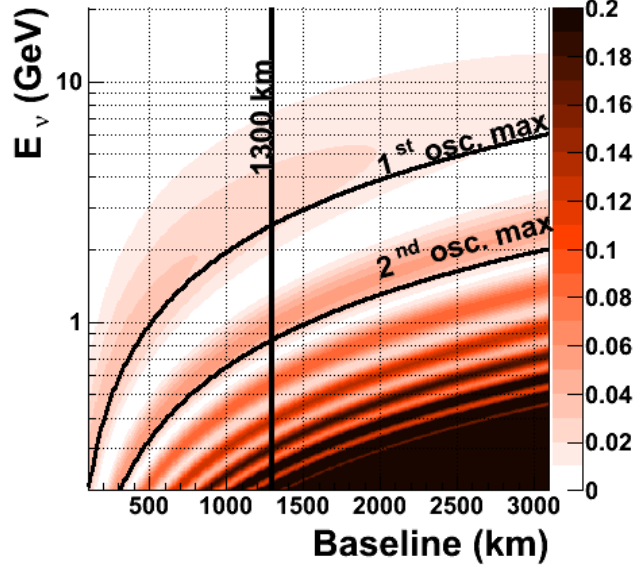
2
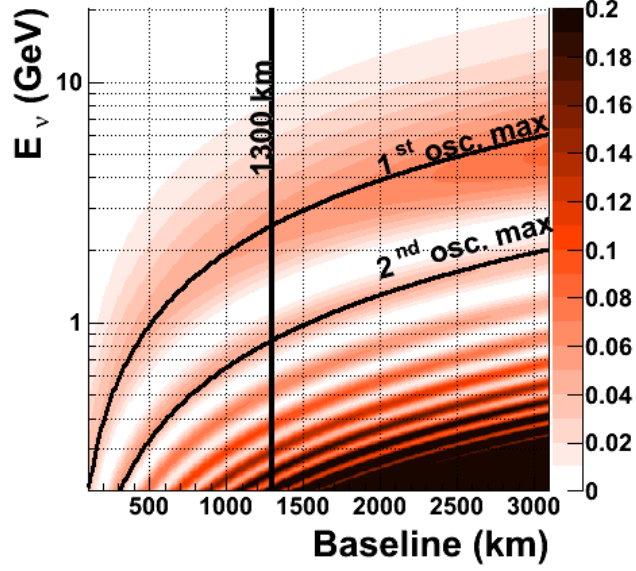
Figure 1: Neutrino oscillations vs energy, baseline and as a function of different values of δ_{cp}. The oscillograms on the left show the $\nu_\mu \to \nu_e$ oscillation probabilities as a function of baseline and energy for neutrinos (top left) and anti-neutrinos (bottom left) with $\delta_{cp} = 0$ and a normal hierarchy. The figures on the right show the projection of the oscillation probability on the neutrino energy axis at a baseline of 1300km for $\delta_{cp} = 0$ (red), $\delta_{cp} = +\pi/2$ (green), and $\delta_{cp} = -\pi/2$ (blue) for neutrinos (top right) and anti-neutrinos (bottom right). The yellow curve is the ν_e appearance solely from the "solar term" due to 1-2 mixing as given by Equation 7.
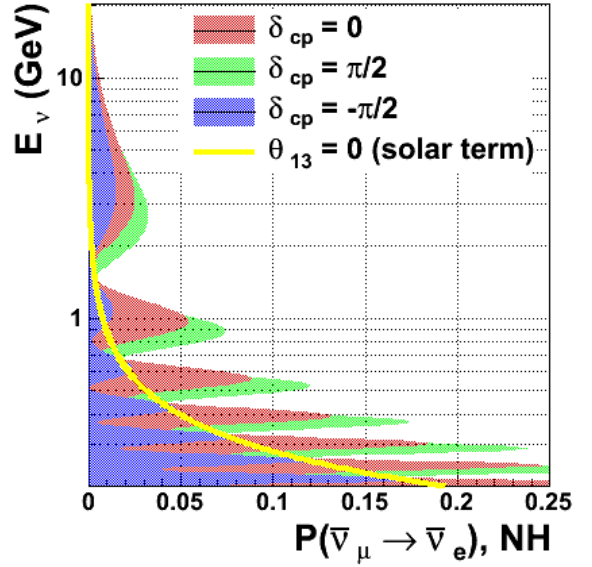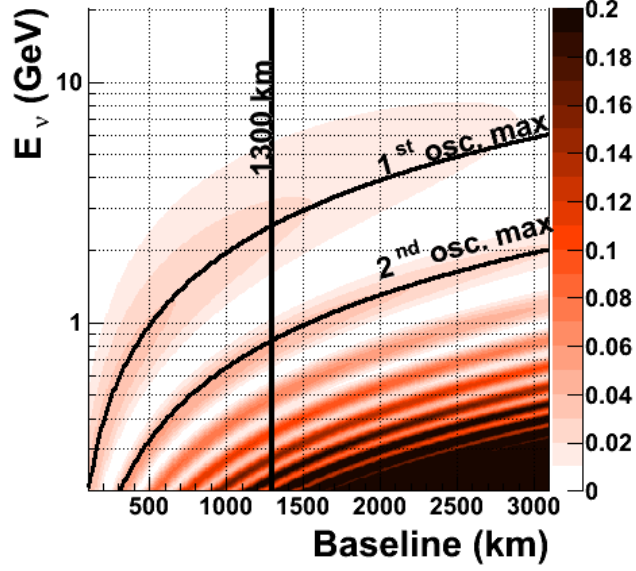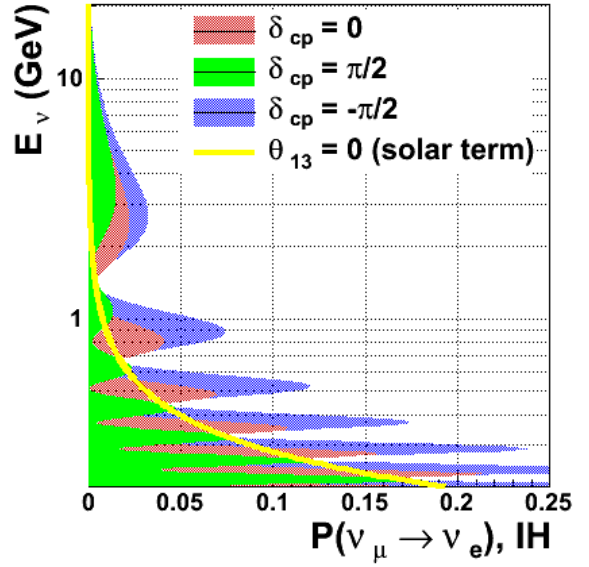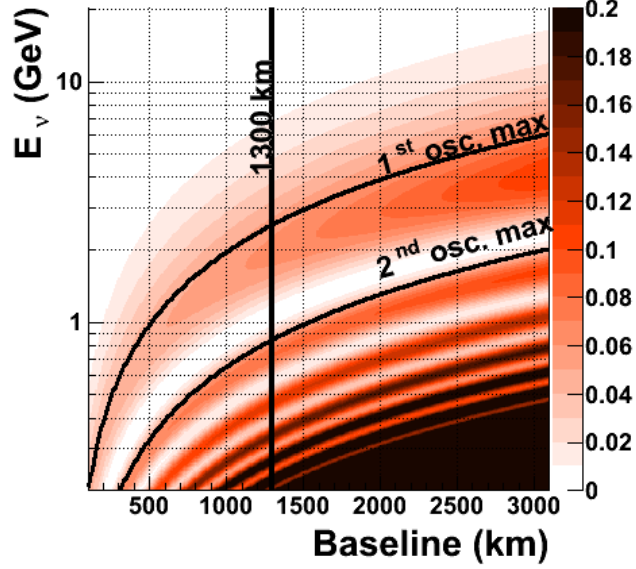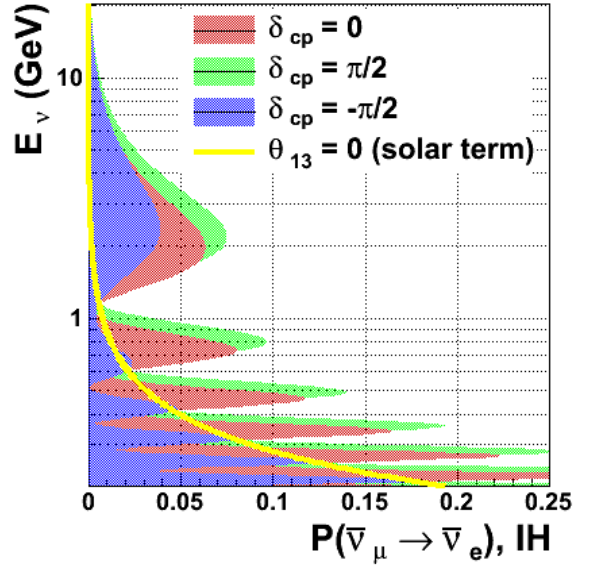
Figure 2: Neutrino oscillations vs energy, baseline and as a function of different values of δ_{cp}. The oscillograms on the left show the $\nu_\mu \to \nu_e$ oscillation probabilities as a function of baseline and energy for neutrinos (top left) and anti-neutrinos (bottom left) with $\delta_{cp} = 0$ and an inverted hierarchy. The figures on the right show the projection of the oscillation probability on the neutrino energy axis at a baseline of 1300km for $\delta_{cp} = 0$ (red), $\delta_{cp} = +\pi/2$ (green), and $\delta_{cp} = -\pi/2$ (blue) for neutrinos (top right) and anti-neutrinos (bottom right).The yellow curve is the ν_e appearance solely from the "solar term" due to 1-2 mixing as given by Equation 7.
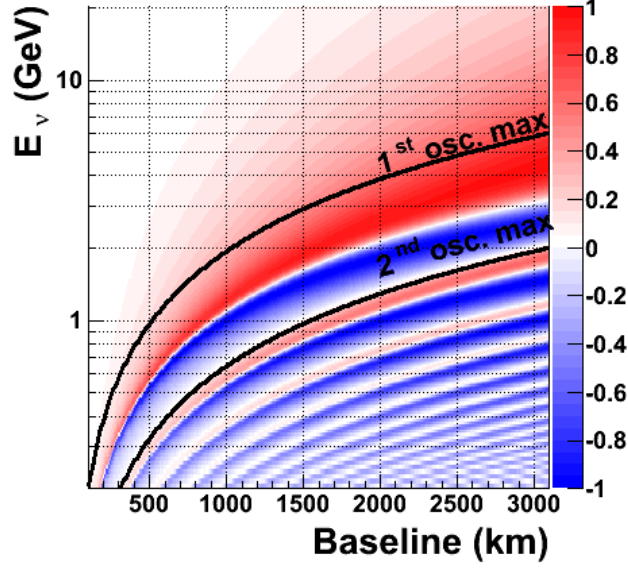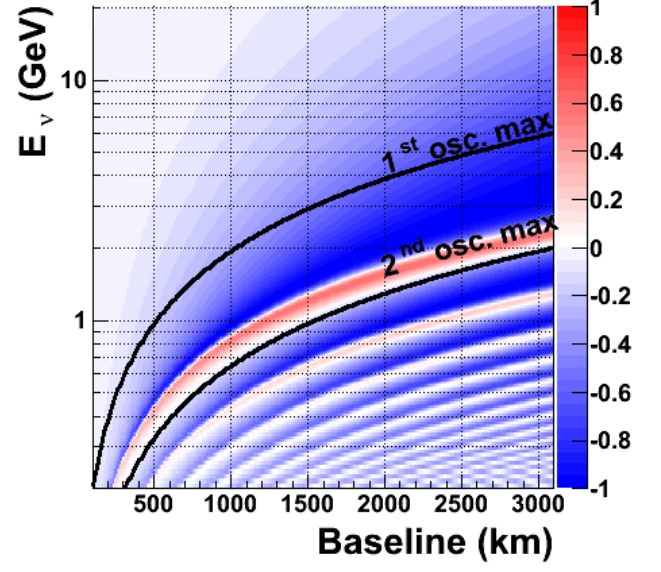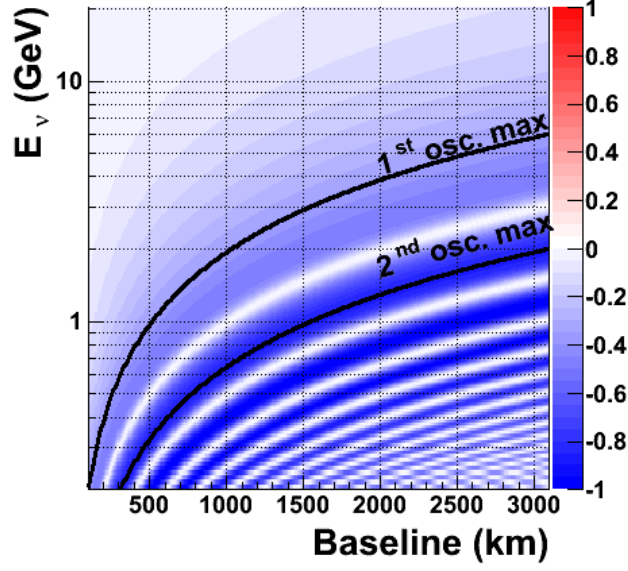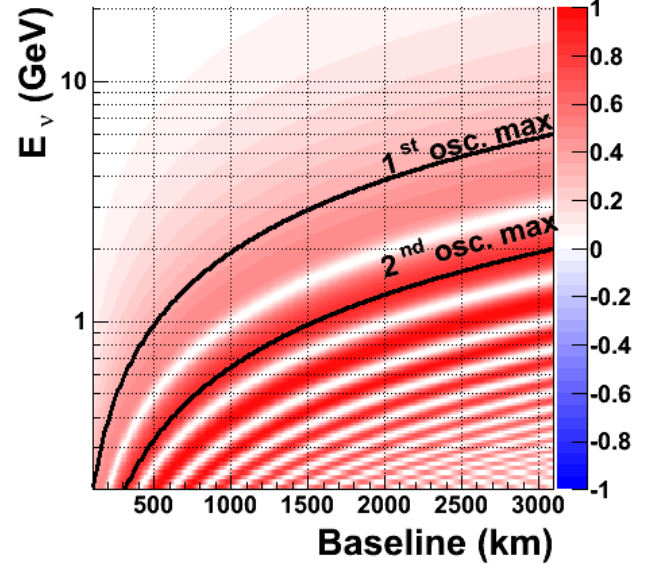
Figure 3: The CP asymmetry as a function of baseline. The top two figures are for the asymmetry induced by the matter effect only for normal (top left) and inverted (top right) hierarchies. The bottom figures are for the asymmetry induced through the CP violating phase δ_{cp} in vacuum, for $\delta_{cp} = +\pi/2$ (bottom left) and $\delta_{cp} = -\pi/2$ (bottom right)

The simple phenomenology of $\nu_\mu \to \nu_e$ oscillations described above implies that the experimental sensitivity to CP violation from measurements of the total asymmetry between $P(\nu_l \to \nu_{l'})$ and $P(\bar{\nu}_l \to \bar{\nu}_{l'})$ necessitates the disambiguation of asymmetries induced by the matter effect and asymmetries induced by CP violation. This is particularly true for experiments using neutrino beams of $\mathcal{O}(1\text{GeV})$ which require baselines of $\mathcal{O}(100\text{km})$ to access the 1-3 mixing scale. At these baselines the matter asymmetries are signficant. We note that the magnitude of the matter asymmetry is calculable within an uncertainty of $< 10\%$ using the currently known values of the oscillation parameters. Only the sign of the asymmetry which depends on the sign of Δm_{31}^2 is unknown. An example of the ambiguities that can arise from the interference of the matter and CP asymmetries is shown in Figure 4. The figures show (clockwise from top left) the total asymmetry as a function of δ_{cp} at baselines of 290 km 810km, 2300km, and 1300km. The curves in black and red are the asymmetries at the 1st and second oscillation nodes respectively. The solid lines are for normal hierarchy and dashed lines are for inverted hierarchy. The figures demonstrate the measurements of the asymmetry at the 1st oscillation node yield ambiguous results for experiments with short baselines if the hierarchy is unknown. This occurs in regions of the (L, E, δ_{cp}) phase space where the matter and CP asymmetries cancel partially or totally. For example the green line in Figure 4 indicates the asymmetry at the first node for maximal CP violation ($\delta_{cp} = \pi/2$) with an inverted hierarchy. At a baseline of 290 km the measured asymmetry ($\delta_{cp} = \pi/2$, inverted hierarchy) is degenerate with ($\delta_{cp} \sim 0$, normal hierarchy) at the first node. Measurements of the asymmetry at at different L/E or at different baselines can break the degeneracies (Equation 15). At very long baselines where the matter asymmetry exceeds the maximal CP asymmetry, there are no degeneracies and the mass hierarchy and CP asymmetries can be resolved in the same experiment. For the current best fit values of the oscillation parameters the degeneracies in measurements at the first oscillation maximum are resolved at a baseline of ~ 1200km.
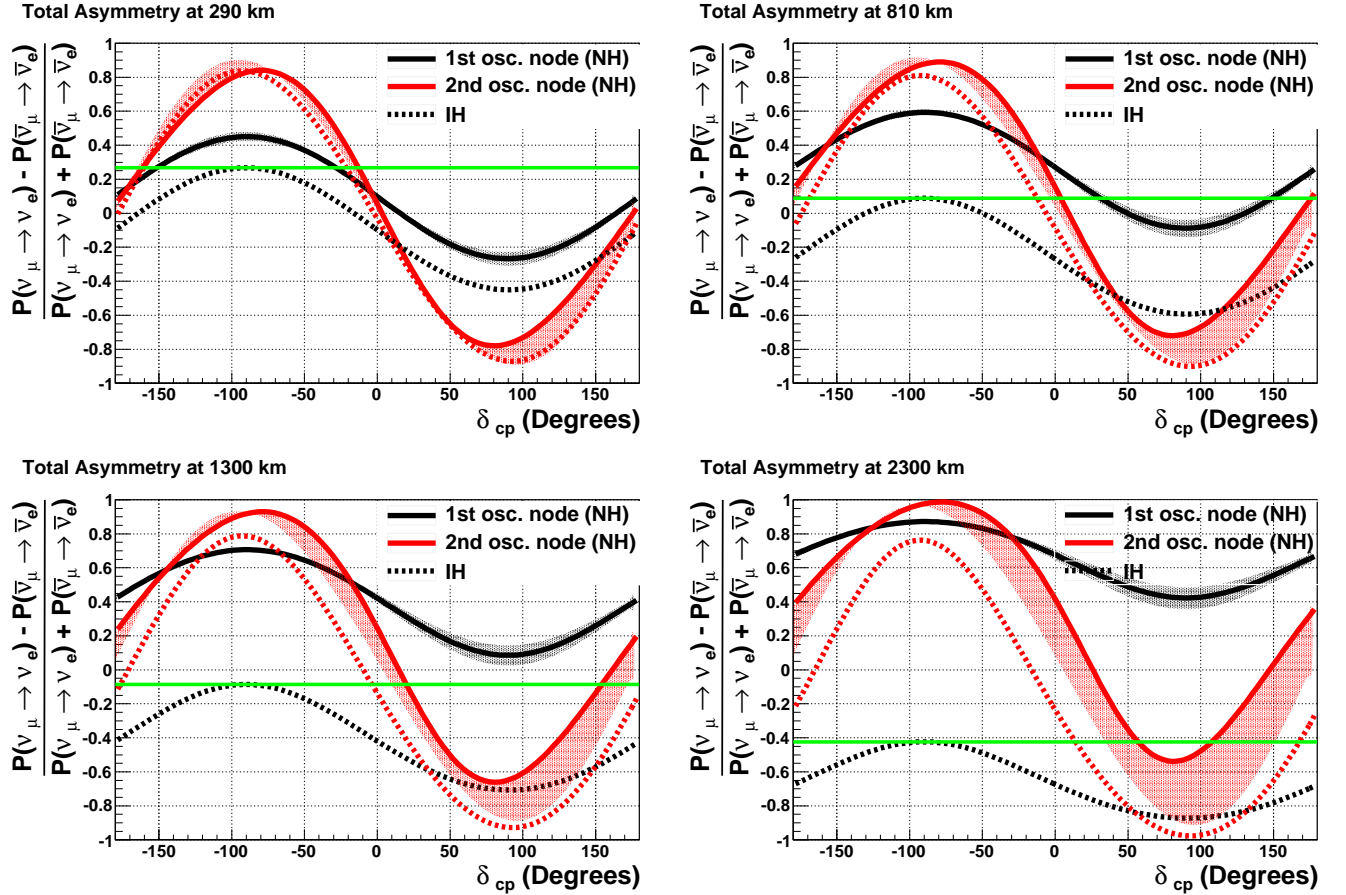

Figure 4: $\nu/\bar{\nu}$ oscillation asymmetries vs δ_{cp} at the first 2 oscillation nodes. Clockwise from top left: 290km, 810km, 2300km,1300km.

2 Experimental Approaches

The general experimental parameters for designing a successful neutrino oscillation experiment to address neutrino CP violation can be extrapolated from the phenomenology summarized in Section 2 as follows:

1. *Phenomenology: An appearance experiment is necessary to extract the CP violating effects.* **Experimental requirements:**

   - The experiment probes oscillations of $\nu_{\mu,e} \rightarrow \nu_{e,\mu}$
   - The flavor of the neutrino at production and after flavor transformations must be tagged or known, therefore the experiment needs to identify ν_e and ν_μ with high efficiency and purity.
   - Flavor tagging of muon neutrinos using the lepton flavor produced in a charged-current interaction such that $\nu_\mu + N \rightarrow \mu N' X$ requires $E_\nu > 100$ MeV.

2. *Phenomenology: In the 3 flavor mixing model, the CP violating Jarlskog invariant arises in the interference term $P_{\sin \delta}$ as given by Equation 8, the oscillation scale where the interference term is maximal is that determined by the mixing between the 1-3 states.* **Experimental requirements:**

   - The experimental baseline and corresponding neutrino energy is chosen according to Equation 11 such that $L/E = 510$ km/GeV to maximize sensitivity to the CP violating term in the neutrino flavor mixing.
   - Flavor tagging of muon neutrinos which can be produced either as the source or after flavor mixing requires $E_\nu > 100$ MeV, therefore, the experimental baselines over which to measure neutrino oscillations are $L > 50$ km. [1]

3. *Phenomenology: In the 3-flavor model $\nu_{\mu,e} \rightarrow \nu_{e,\mu}$ oscillations depend on all parameters in the neutrino mixing matrix as well as the mass differences as shown in Equations 5 to 8.* **Experimental requirements:**

   - The precision with which δ_{cp} can be determined - and the sensitivity to small CP violating effects or CP violation outside the 3-flavor model - requires precision determination of all the other mixing parameters - preferably in the same experiment.

4. *Phenomenology: Evidence for CP violation necessitates the explicit observation of an asymmetry between $P(\nu_l \rightarrow \nu_{l'})$ and $P(\bar{\nu}_l \rightarrow \bar{\nu}_{l'})$.* **Experimental requirements:**

   - The experiment must probe the oscillations of both neutrinos and anti-neutrinos in an unambiguous way.
   - Charge tagging in addition to flavor tagging is required. Charge tagging can be achieved at detection using the lepton charge and/or at production by selecting beams of pure neutrinos or anti-neutrinos.
   - The mass hierarchy is as yet undetermined. The experiment must be designed to resolve degeneracies between the matter and potential CP asymmetries. This can be achieved by using a baseline of > 1200 km or with measurements probing oscillations over different L/E.

5. *Phenomenology: CP asymmetries are maximal at the secondary oscillation nodes.* **Experimental requirements:**

   - Coverage of the L/E scale of the secondary oscillation nodes improves experimental sensitivity to small values of δ_{cp} by enabling measurements of the asymmetry at the secondary nodes where the CP asymmetries are much larger and where there are no degeneracies with the matter asymmetries.
   - The secondary oscillation nodes are located at scales set by Equation 11 where $n > 1$. The second oscillation maxima is located at scales given by $L/E \sim 1500$ km/GeV. If muon flavor tagging at production and/or detection, the experimental baseline is required to be > 150 km.

2.1 Neutrino Sources

To fulfill the experimental requirements of a ν CP violation experiment described earlier, an appropriate source of $\nu_{\mu,e}$ is needed. There are two main sources of neutrinos that can be used; atmospheric neutrinos and neutrino beams produced from high power proton accelerators. There are three main techniques for producing neutrinos from a proton accelerator that are sketched out in Figure 5 and summarized below:

---

[1] Neutrino experiments using beams from pion decay-at-rest experiments such as DAEδUS are an exception since the $bar\nu_\mu$ production spectrum is well known and only the $\bar{\nu}_e$ flavor after oscillations is tagged through inverse beta decay. The neutrino energies are ~ 50 MeV below the CC muon production threshold.
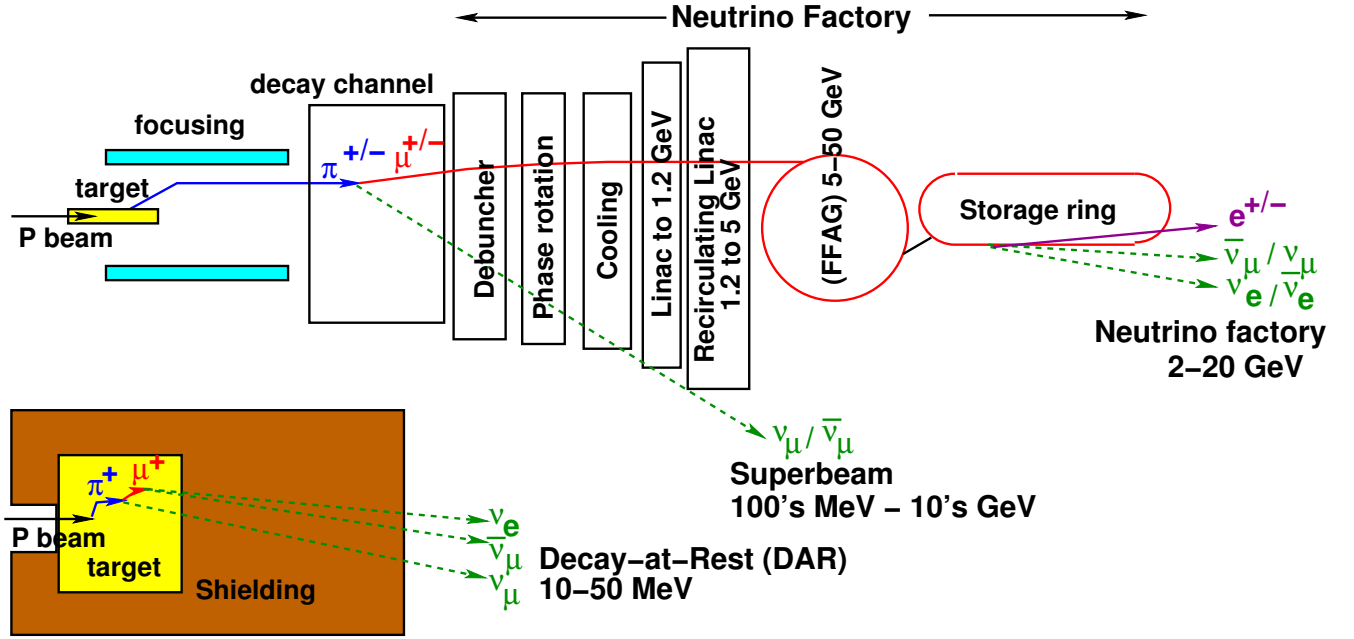
Figure 5: Schematic demonstrating production of accelerator neutrino beams from a high power proton accelerator. The conventional neutrino beam - called a Superbeam - shares a similar front end to a neutrino factory.

Conventional horn-focused neutrino beams: A proton beam is directed at a thin solid target of several nuclear interaction lengths. Hadrons, primarily $\pi^{\pm}$ and $K^{\pm}$ produced within the target target and escape. The target is placed in the vicinity of a series of consecutive magnetic focusing horns. Depending on the current polarity, the horns will preferentially focus positive or negative hadrons. The hadrons travel through an evacuated decay channel where they decay primarily to ν_{μ}. Horn focusing works best for hadrons with energies ≥ 1 GeV.

PROS:

- The technology has been used since the 1960's and is technically very mature and well understood.

- Horn focused beams are highly tunable, by varying the proton beam energy, target and horn placement, a different range of hadron momenta can be focused to produce wide-band on-axis neutrino beams with peak energies from 100's MeV to 10's of GeV. Lower energy neutrino beams (100's MeV) are produced from horn focused beams by placing the detectors off-axis. Figure 6 demonstrates the versatility of horn focused beams. Beams matched to the oscillation patterns at baselines of 300km, 1300km and 2500km are shown. The beams cover all of the first oscillation node and at the longer baselines part of the second.

- The asymmetry in $\nu_{\mu}/\bar{\nu}_{\mu}$ is probed directly over a range of L/E that covers most of the first and some of the second oscillation maxima as required.

CONS:

- Horn focused beams can focus only a small fraction of the pions produced from the proton beam interactions in the target. Primarily hadrons > 1 GeV. Only one polarity is focused at a time.

- The main drawback of a ν_{μ} horn focused beam is the presence of a small ν_e contaminant (from kaon and muon decays) which is typically $\sim 1\%$ [10]. This introduces an irreducible background to the ν_e appearance search. Given the current values of the oscillation parameters, the oscillation probability at the first maximum is $P^{\text{vacuum}}(\nu_{\mu} \to \nu_e)(E_1) \sim \sin^2\theta_{23}\sin^2 2\theta_{13} \sim 5\%$ so the appearance signal is significantly larger than the irreducible ν_e background.

- There is a wrong sign contaminant in the muon neutrino beam from unfocused wrong sign hadrons. The wrong sign ν_{μ} component is typically $\sim 7\%$ [10]. This is not a problem for ν_{μ} oscillations but the wrong sign component is $\sim 30\%$ of the $\bar{\nu}$ beam spectrum due to the lower anti-neutrino cross-sections and smears out the asymmetry. A new target design employing high-Z materials is under study that could potentially reduce the wrong sign component in the $\bar{\nu}$ beam to $\sim 15\%$ of the spectrum.

- The precision determination of the absolute neutrino flux, the flavor content and energy distribution of a horn focused beam requires the deployment of high precision near detectors, external measurements of hadron production from the target, and precision modeling of the horn focusing. Current ν_e appearance experiments have produced predictions of the un-oscillated flux of 10% with no near detector [12] and $\sim 7\%$ with a near detector [11].

Pion Decay-At-Rest High power proton beams targeted at a large dump produce π^+ which stop and decay at rest to μ^+ and a mono-energetic muon neutrino with an energy of 28 GeV. The μ^+ is captured and decays producing a $\nu_e, \bar{\nu}_\mu$ pair. Since the muon decays are polarized, the shape of the ν_e and $\bar{\nu}_\mu$ spectra are distinct with $\bar{\nu}_\mu$ peaking at higher energy as shown in Figure 6. Neutrino beams from a DAR experiment peak at 52 MeV and are used in short baseline experiments. A proposal to search for CP violation using oscillations of $\bar{\nu}_\mu \rightarrow \bar{\nu}_e$ in a DAR experiment has been developed [13]. The design utilizes several low-cost, high-power proton accelerators under development for commercial uses. The design requires several cyclotrons deployed at different baselines from a massive scintillator or Gd-doped water detector.
PROS:

- The technique has been used since the 1980's and is well understood.
- The shape of the $\nu_e, \bar{\nu}_\mu$ spectrum is calculable from first principals and the $\nu_e \rightarrow \nu_e$ spectrum can be used to obtain the absolute flux normalization.

CONS:

- In order to measure the $\bar{\nu}_\mu \rightarrow \bar{\nu}_e$ over a range of L/E to determine the value of δ_{cp}, the proposal is to deploy of 3 high powered cyclotrons at 3 different baselines from a massive liquid scintillator detectors. The technology to develop these "portable" 1MW cyclotrons is still in the R&D stage.
- To get the desired sensitivity requires the experiment to be coupled to a long baseline conventional neutrino beam.
- Can not probe direct CP violating asymmetries in $\nu_\mu/\bar{\nu}_\mu$ oscillations.

Neutrino Factories The front end of a neutrino factory is very similar to a conventional neutrino beam. A target is bombarded with a high power proton beam, the pions produced are focused into a decay channel. The current design of the neutrino factory [14] utilizes large superconducting solenoids to focus both π^+ and π^- into a decay channel. The solenoid captures a much larger fraction of the pions produced by the proton beam than horn focusing. In the current staging of the neutrino factory a horn focused beam is used in the first stage, and solenoid focusing is used in later stages. The muons produced from the decay of pions are captured, bunched, and manipulated in 6-D phase space then cooled (the first stage of the NF does not utilize cooling) and transported into an accelerator chain. There are at least three acceleration stages envisioned: a linear accelerator, followed by a recirculating linac followd by a by a Fixed-Field Alternating Gradient (FFAG) synchrotron. The current NF designs accelerate muons to energies from 5 to 50 GeV. The muons are extracted from the FFAG and injected into a racetrack shaped storage ring with two straight sections where they decay $\mu^+ \rightarrow e^- \nu_e \bar{\nu}_\mu$. With solenoid focusing at the front end, the NF is designed to collect and store both muon polarities simultaneously.
PROS:

- The neutrino flux is known to $\sim 1\%$
- The asymmetry in $\nu_e/\bar{\nu}_e$ oscillations is probed directly over a range of L/E.
- The NF collects and stores both polarities of muons in the storage ring at the same time. This implies that $\nu_e/\bar{\nu}_e \rightarrow \nu_\mu/\bar{\nu}_\mu$ oscillations can be probed simultaneously using a magnetized far detector.
- The beam contains equal parts ν_e and the opposite polarity ν_μ from muon decays, so in principal $\nu_e/\bar{\nu}_e \rightarrow \nu_\mu/\bar{\nu}_\mu$ and $\nu_\mu/\bar{\nu}_\mu \rightarrow \nu_e/\bar{\nu}_e$ oscillations can be probed in the same experiment. This is a unique feature of experiments based at neutrino factories.

CONS:

- Muon cooling is necessary to collect enough muons for long baseline neutrino beams. While the first stage of a neutrino factory does need cooling, it cannot generate enough neutrinos per proton to be competitive with conventional neutrino beams. The numbers of muons collected to make a NF feasible is 2-3 orders of magnitude beyond the current state of the art - the mu2e experiment **??** and hasnt been demonstrated yet.

- The technical challenges to mount an NF are daunting. Every step in the chain from the target and focusing station, the cooling channel, the debuncher...etc, is still under intensive R&D. The timescale for completion of the R&D could be a decade or more and the cost will be large.

- To realise the full physics potential of the NF requires massive magnetized far detectors that can identify both muon and electron charge. The detector technology needed (magentized 100kton LAr-TPC for example) to utilize the beam has also not been demonstrated.

2.1.1 Summary of Event Rates from Neutrino Sources

The total number of appearance events expected from a neutrino source as a function of baseline is given as

$$N_{\nu_e}(L) = \int \Phi(E,L) \times \sigma(E) \times P^{\nu_\mu \to \nu_e}(E,L) \Delta E \tag{16}$$

where $\Phi(E,L)$ is the beam flux as a function of energy and baseline and $\sigma(E)$ is the total neutrino cross-section. If we assume $\delta_{cp} = 0$, vacuum oscillations only and assume that the neutrino beam source produces a wide coverage that is flat in energy in the oscillation region then

$$\Phi(E,L) = \frac{C}{L^2} \tag{17}$$

$$\sigma(E) = 0.67 \times 10^{-38} (\text{cm}^2/\text{GeV}/N) \times E \tag{18}$$

$$P^{\nu_\mu \to \nu_e}(E,L) = \sin^2 \theta_{23} \sin^2 2\theta_{13} \sin^2 (1.27 \Delta m_{31}^2 L/E). \tag{19}$$

$$\tag{20}$$

By plugging in the above values into Equation 16 we find that

$$N_{\nu_e}(L) = A \int \frac{\sin^2(ax)}{x^3} dx, \quad x = L/E, \quad a = 1.27 \Delta m_{31}^2 \tag{21}$$

The integral of Equation 21 over the first two nodes is a constant that is largely independent of baseline for baselines > 300km. The event rate at experiments with baselines < 300 km are lower because the neutrino cross-sections < 0.5 GeV are no longer linear with energy.

The following simple arguments demonstrate why exposures of order several 100's kilo-ton × mega-watt × years are needed to reach 5σ CP violation sensitivities over at least 50% of the allowed values of δ_{cp} regardless of the neutrino source and experimental approach:

1. If we naively assume the neutrino source can generate a flat spectrum of $1 \times 10^{17} \nu/\text{GeV}/\text{m}^2/\text{MW.year}$ at 1 km [2], then integrating Equation 16 over the region of the first two oscillation nodes yields:

$$N_{\nu_e}^{\text{appear}}(L) = \int_{E_0 = L\Delta m^2/2\pi}^{10 \times E_0} \Phi(E,L) \times \sigma(E) \times P^{\nu_\mu \to \nu_e}(E,L) \Delta E \sim \mathcal{O}(10) \text{ events}/(\text{kT.MW.yr}) \tag{22}$$

where E_0 is the lower end of the 2nd oscillation node.

2. The appearance rate is roughly constant for baselines > 300 km with no matter effects. For shorter baselines the event rates are lower since neutrino cross-sections are no longer linear with energies for $E < 0.5$ GeV.

3. The $\bar{\nu}_e$ appearance event rate is $\sim 1/2$ that of ν_e due to the lower cross-sections for $E > 1$ GeV.

4. The maximal CP asymmetry at the first oscillation node is around 30%. Although the maximal asymmetry at the second oscillation node is 80%. the contribution of the secondary oscillation nodes to the observable asymmetry is reduced due to the decrease in neutrino cross-section as the energy decreases.

The real event yields from several current and proposed experiments are summarized in Table 1 and are consistent with the arguments presented above.

The low rate of ν_e appearance illustrates the challenges of designing an experiment to reach 5 σ sensitivity to CP violation in neutrinos over a significant range of δ_{cp} values. The current generation of high intensity proton accelerators that are capable of producing the appropriate neutrino beams operate at < 1 MW of power. The proposed Project X proton driver project will further increase the beam power from the Fermilab accelerator complex to several MW as summarized in Table 2. Other worldwide sources of high intensity proton accelerators are summarized in Table 3.

---

[2]The number is based on the NuMI beam performance on-axis with 1 year = 2×10^7 seconds such that 1 MW.yr = 10^{21} 120 GeV protons on target.

Table 1: Raw ν oscillation event rates at the far site (no detector effects) with $E_\nu < 10$ GeV. Assumes 1.65×10^7 seconds/year (Fermilab) unless otherwise noted. Oscillation parameters are: $\theta_{12} = 0.587$, $\theta_{13} = 0.156$, $\theta_{23} = 0.670$, $\delta m^2 = 7.54 \times 10^{-5} eV^2$, and $\Delta m^2 = 2.47 \times 10^{-3} eV^2$. The NC event rate is for events with visible energy > 0.5 GeV except in the case of T2K where the event rate for NC is given for $E_{vis} > 0.25$ GeV. The event rate is given for ≈ 50 kt.yrs. The beam power varies for each facility. For later stages of the neutrino factories we note that both beam polarities can run simultaneously.

Superbeam	ν_μ unosc. CC	ν_μ osc. CC	ν_e beam CC	ν_μ NC	$\nu_\mu \to \nu_\tau$ CC	$\nu_\mu \to \nu_e$ CC $\delta_{CP} = -\pi/2$	$0,$	$\pi/2$
T2K: 295 km 30 GeV, 750 kW 9×10^{20} POT/year note: duty factor $\sim$1/3 of NuMI/LBNE								
50 kt-years ν	2100	898	41	360	< 1	73	58	39
MINOS: 735 km 120 GeV, 700 kW 6×10^{20} POT/year LE Beam								
50 kt-years ν	17574	11223	178	4806	115	345	326	232
50 kt-years $\bar{\nu}$	5607	3350	56	2017	32	58	85	88
NOvA: 810 km 120 GeV, 700 kW 6×10^{20} POT/year								
50 kt-years ν	4676	1460	74	1188	10	196	168	116
50 kt-years $\bar{\nu}$	1388	428	19	485	2	22	35	41
LBNE: 1300 km 80 GeV, 700 kW 9×10^{20} POT/year								
50 kt-years ν	7421	2531	63	1953	91	353	280	204
50 kt-years $\bar{\nu}$	2478	812	20	876	28	30	50	62
LBNO: 2300 km 50 GeV, 485 kW 1×10^{21} POT/year								
50 kt-years ν	2851	824	16	818	190	178	142	112
50 kt-years $\bar{\nu}$	1022	276	4	380	85	8	15	18
Neutrino Factory	ν_μ unosc. CC	ν_μ osc. CC		ν_μ NC	$\nu_\mu \to \nu_\tau$ CC	$\nu_e \to \nu_\mu$ CC $\delta_{CP} = -\pi/2$	$0,$	$\pi/2$
NF Stage 1 3 GeV, 1MW no cooling 0.94×10^{20} μ decays/year								
50 kt-years μ^+	1039	339		484	28	71	97	117
50 kt-years μ^-	2743	904		945	89	24	19	12
NF Stage 2 3 GeV, 3MW 5.6×10^{20} μ decays/year								
50 kt-years μ^+	6197	2018		2787	300	420	580	700
50 kt-years μ^-	16349	5390		5635	534	139	115	85

Table 2: The current and future experimental research programs planned for the Fermilab accelerator complex.
* Operating point in range depends on Main Injector (MI) energy for neutrinos.
** Operating point in range depends on MI inject or slow-spill duty factor (df) for kaon program.

		PROJECT X			
Program	2013	Stage 1 (2025 ?)	Stage 2	Stage 3	Stage 4
Description	NOνA	1 GeV CW linac	3 GeV CW linac	RDR	beyond RDR
MI Neutrinos	470-700 kW	515-1200 kW	1200 kW	2450kW	2450-4000 kW
8 GeV neutrinos	15 kW+0-50kW**	0-42kW+0-90 kW**	0-84 kW*	0-172 kW*	3000kW
8 GeV Muons	20 kW	0-20 kW*	0-20 kW*	0-172 kW*	1000 kW
1-3 GeV Muons	—	80 kW	1000 kW	1000 kW	1000 kW
Kaons	0-30 kW**	0-75 kW**	1100 kW	1870 kW	1870 kW
	($< 30\%$ df from MI)	($< 45\%$ df from MI)			
Nuclear edm ISOL	none	0-900 kW	0-900 kW	0-1000 kW	0-1000 kW
Ultra-cold neutrons	none	0-900 kW	0-900 kW	0-1000 kW	0-1000 kW
Nuclear technology	none	0-900 kW	0-900 kW	0-1000 kW	0-1000 kW
# Programs	4	8	8	8	8
Total max power	735 kW	2222 kW	4284 kW	6492 kW	11870kW

Table 3: High intensity Accelerator Programs Current and Planned in the US and Worldwide

| Facility	Location/Region	Proton energy	Power	Duty Cycle	Status
Fermilab MI	U.S.	60-120 GeV	520 - 700 kW	$\sim 1.7 \times 10^7$ seconds/yr	Starts 2013
Project X	U.S.	8-120 GeV	3 - 2.4 MW		See Table 2 for details
SNS	U.S.	0.8 GeV	1MW		No neutrino program
J-PARC	Japan	30 GeV	750 kW	$\sim 0.6 \times 10^7$ seconds/yr	upgrade in ??
J-PARC	Japan	50 GeV	1.66 MW		T2HK proposal
CERN SPS	CERN	400 GeV	700kW	$\sim 1.5 \times 10^7$ seconds/yr	available in ??
CERN HP-PS	CERN	50 GeV	2MW	$\sim 1.5 \times 10^7$ seconds/yr	Proposed
ESS	Sweden	2.5 GeV	5MW		Construction ~ 2014
Protvino	Russia	70 GeV	450kW	$\sim 1 \times 10^7$ seconds/yr	
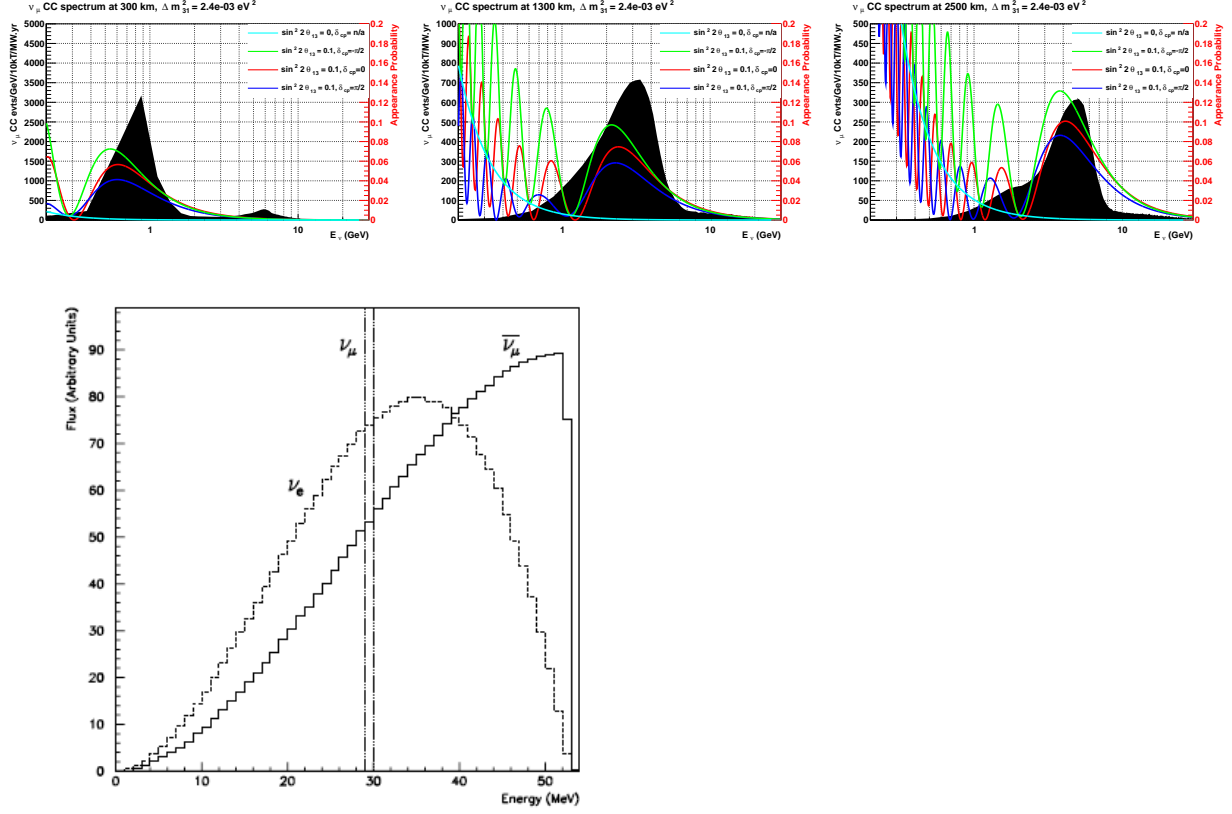
Figure 6: Top:Conventional horn focused beam spectra (un-oscillated) are shown as black histograms overlaid with the colored curves indicating the ν_e appearance probabilities for different values of δ_{cp} at 3 different baselines: 300km (left), 1300km (middle), 2500km (right). Bottom left: the neutrino flavor content and energy spectrum produced from a pion decay-at-rest source. Bottom right: neutrino energy spectrum produced from a 5 and 10 GeV neutrino factory

2.1.2 Atmospheric Neutrino Sources

The latest calculations of the atmospheric neutrino flux for 3 different proposed neutrino detector locations [16] is shown in Figure 7. Atmospheric neutrinos can probe oscillations over baselines of a few 100 km (the ionosphere) to around 13,000 km (the earths diameter). Sensitivity to CP violation using atmospheric neutrinos requires precision determination of both the energy and the direction (to determine the baseline) of the incoming neutrino as well as the determination of the flavor. The estimates of the atmospheric neutrino flux strongly depends on location due to the variation in the earths magnetic field [16]. The models of the flux of atmospheric neutrinos are not accurate enough to estimate the unoscillated spectrum, therefore combinations of measurements over multiple L/E are used to extract the neutrino oscillation parameters. The biggest challenge with atmospheric neutrinos is the event rate per kiloton of detector is tiny compared to an accelerator source. For example, the NuMI beamline operating at 700 kW produces a beam flux of $\sim 92\%$ ν_μ on-axis at 1km from the target of $6 \times 10^9 \mathrm{m}^{-2}\mathrm{GeV}^{-2}\mathrm{sec}^{-1}$ at 3 GeV (the RMS of the beam is $\approx 20-30$ m at 1 km). Therefore, while CP violating effects can be detected using atmospheric neutrinos in high resolution mega-ton scale detectors, the sensitivity is much less than with a beam neutrino experiment and is at best a complementary measurement.
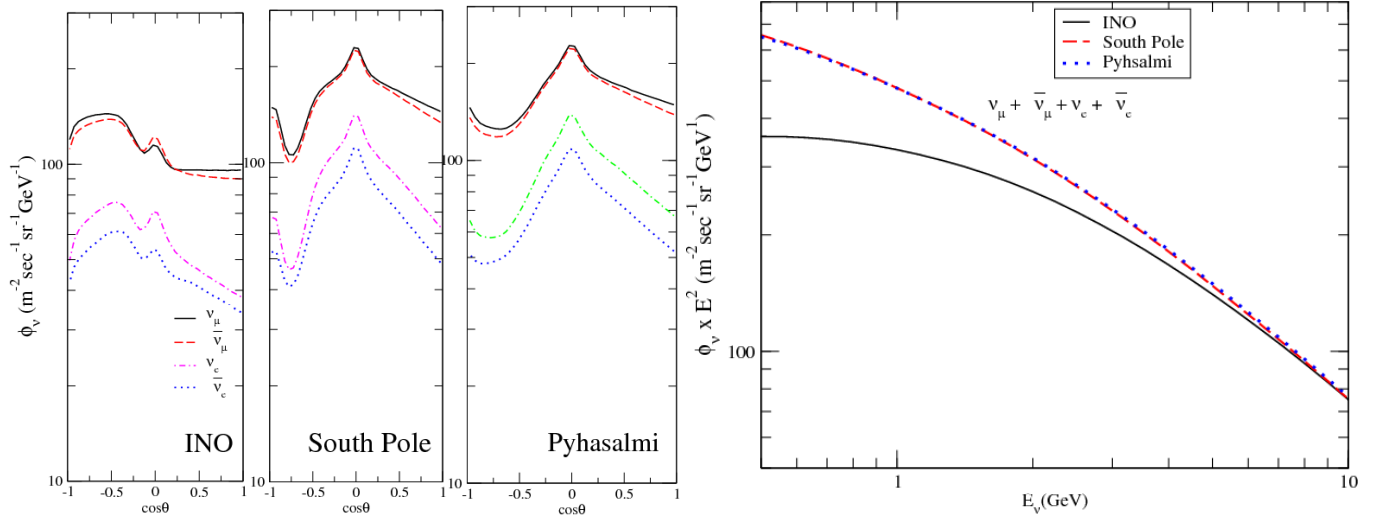

Figure 7: The atmospheric neutrino flux as a function of zenith angle for 1 GeV neutrinos (left) and as a function of energy integrated over all zenith and azimuth angles (right) calculated at 3 different proposed neutrino detector locations from reference [16].

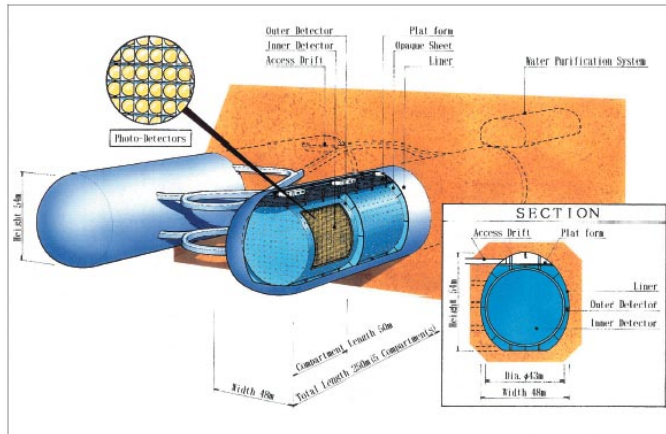## 2.2 Neutrino Detector Technologies

Water Cherenkov Detectors

GD-loaded Water Cherenkov Detectors

Magentized Iron Detectors

Totally Active Scintillator Detectors

Liquid Argon Time-Projection-Chamber
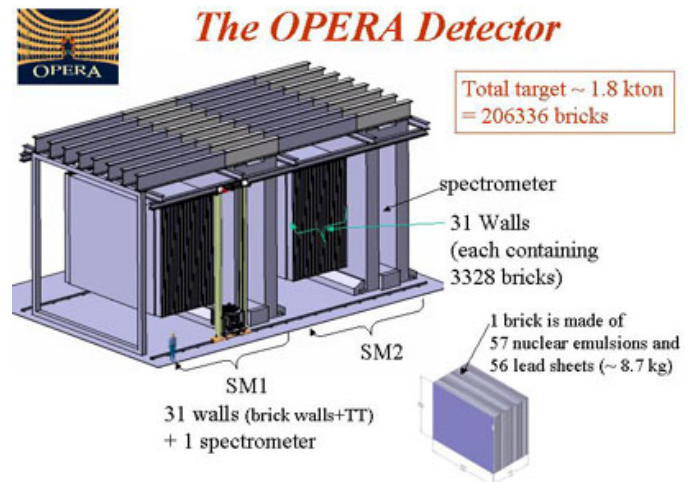
Emulsion detectors

LAr40 Cavern 4850L

Cryogenics – cold box, buffer storage

Cryostat septum
LAr filtration system

HVAC

Detector module
2 high x 3 wide x 18 long drift cells x 2 modules
216 APAs, 224 CPAs

67 m

15.7 m

15.7 m

DETECTOR LAYOUT

Cavern
height: 115 m, diameter: 50 m
shielding from cosmic rays: ~4,000 m.w

Muon Veto
plastic scintillator panels (on top)
Water Cherenkov Detector
1,500 phototubes
100 kt of water
reduction of fast
neutron background

Steel Cylinder
height: 100 m, diameter: 30 m
70 kt of organic liquid
13,500 phototubes

Buffer
thickness: 2 m
non-scintillating organic liquid
shielding external radioactivity

Nylon Vessel
parting buffer liquid
from liquid scintillator

Target Volume
height: 100 m, diameter: 26 m
50 kt of liquid scintillator

vertical design is favourable in terms of rock pressure and buoyancy forces

The OPERA Detector

Total target ~ 1.8 kton
= 206336 bricks

spectrometer

31 Walls
(each containing
3328 bricks)

1 brick is made of
57 nuclear emulsions and
56 lead sheets (~ 8.7 kg)

SM2

SM1

31 walls (brick walls+TT)
+ 1 spectrometer

coil
(3 segments)
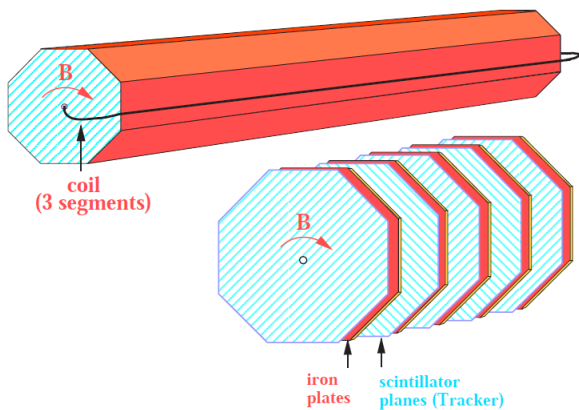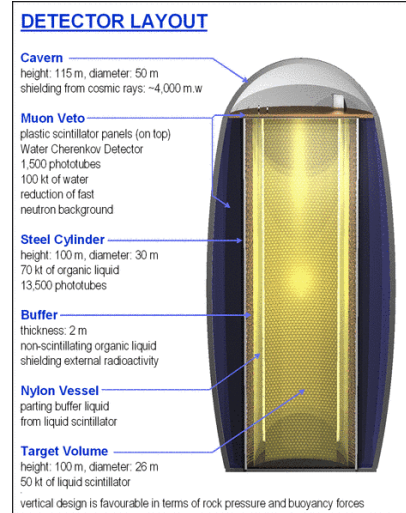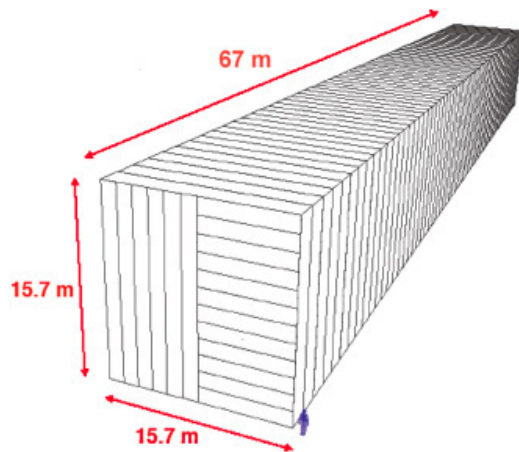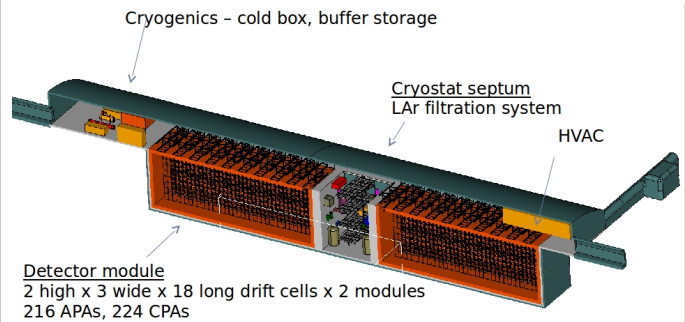
B

B

iron
plates

scintillator
planes (Tracker)

Figure 8: Examples of different massive neutrino detector technologies

15

Table 4: Comparison of different neutrino detector technologies used in long baseline oscillation experiments.

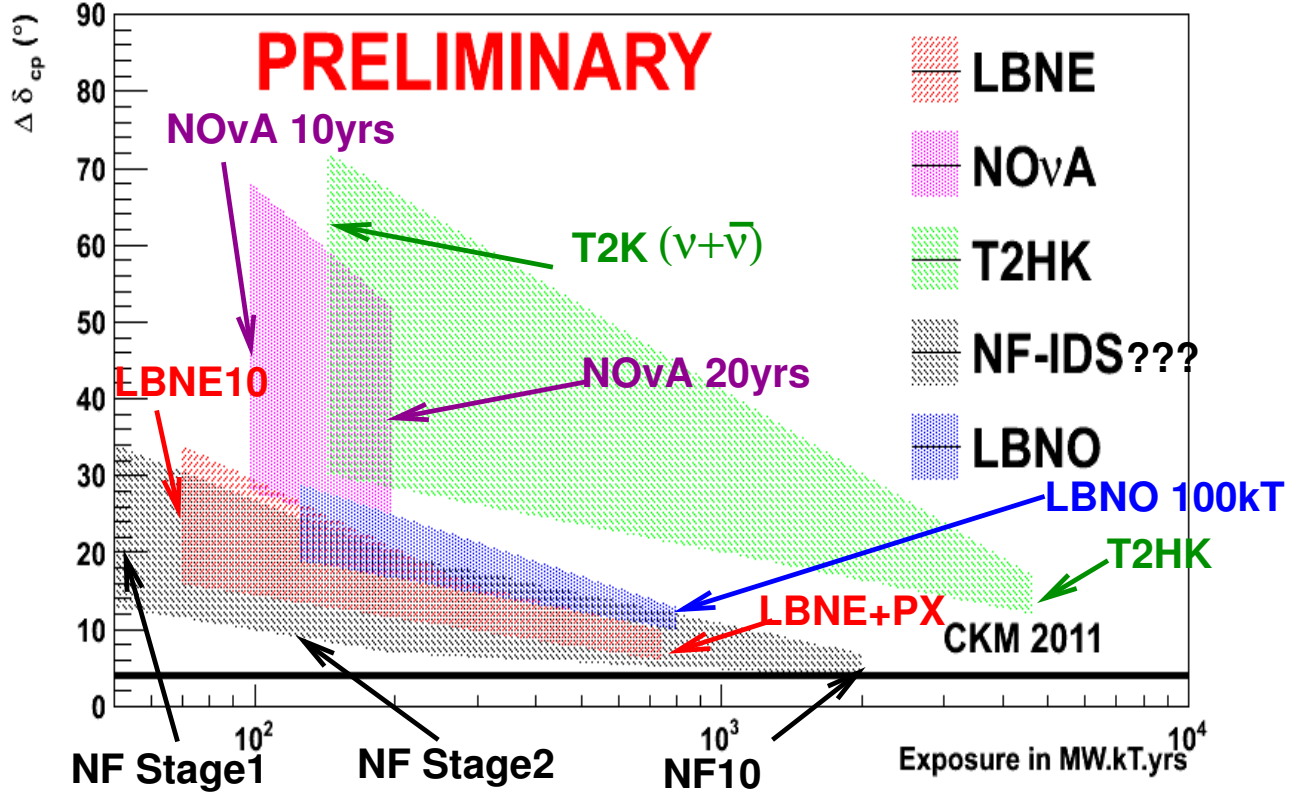| Technology	Cost/10kTon FY12 $	Scalability	μ/e charge selection	ν_μ eff	ν_e eff	ν_τ eff
LAr-TPC	~ 200 \$M	50 kton	N	$\geq 80\%, E_\nu > 0.5$ GeV	$\geq 80\%, E_\nu > 0.5$ GeV	moderate
TASD	~ 150 \$M	100 kton	N	$\geq 60\%, E_\nu > 1$ GeV	$\geq 60\%, E_\nu > 1$ GeV	low
WCD	~ 30 \$M	Mton	N	$\geq 80\%, E_\nu < 1$ GeV	$\geq 80\%, E_\nu < 1$ GeV	v. low
				$\leq 20\%, E_\nu > 2$ GeV	$\leq 20\%, E_\nu > 2$ GeV	
Ice	v. cheap	1000 Mton		> 100 GeV	low	low
MIND	~ 30 \$M	100 kton	Y	$\geq 70\%, E_\nu > 1$ GeV	v. low purity	v. low
Emulsion	???	unknown	few kton ??	excellent	excellent	excellent

Figure 9: Resolution on δ_{cp} as a function of exposure in kt.MW.yr where a year is assumed to be 2e7 seconds for different experimental approaches. The band represents the range of resolutions which varies with the value of δ_{cp}.
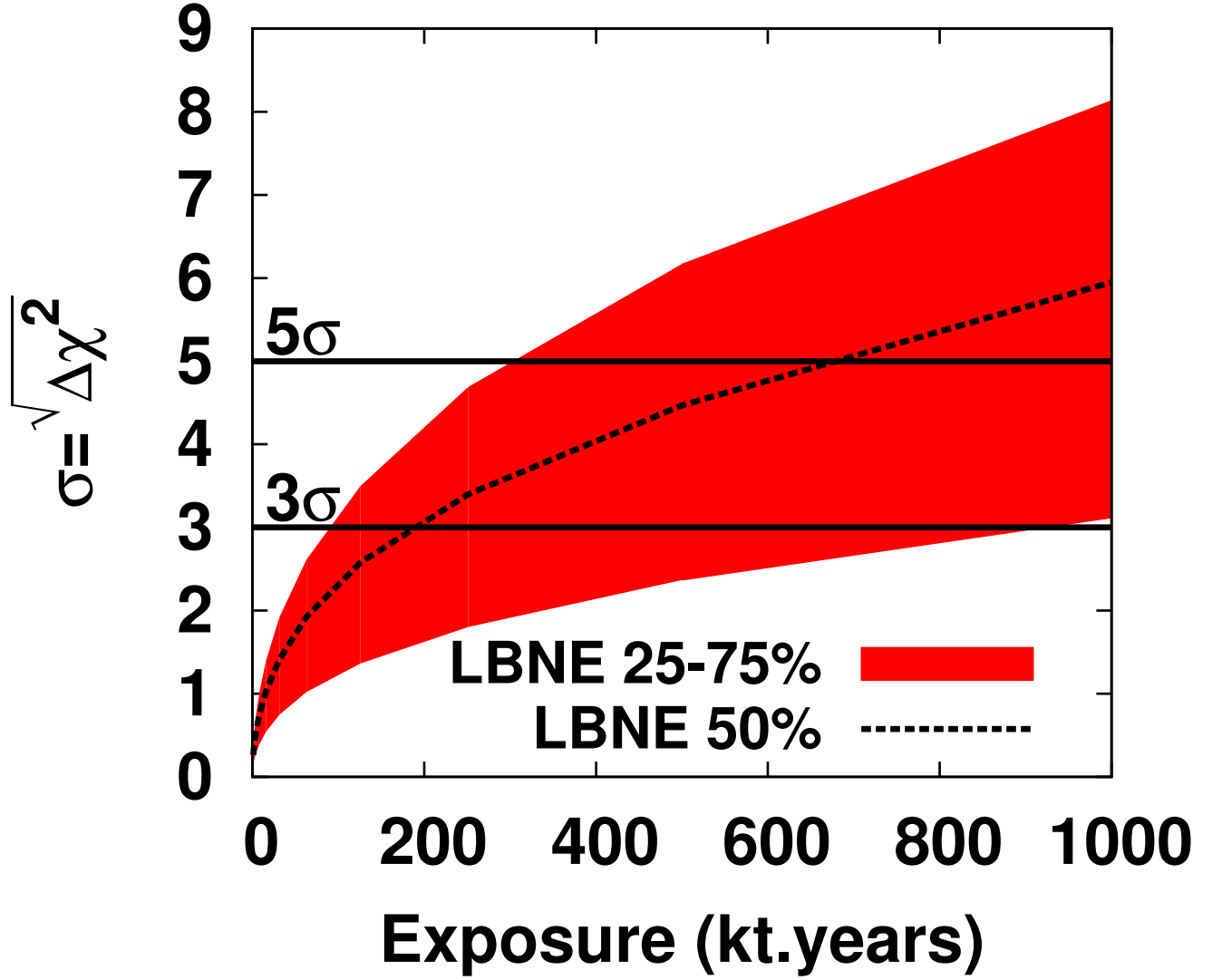
Figure 10: CP violation sensitivity as a function of exposure in LBNE (top). The band represents the sensitivity for 25% to 75% of $delta_{cp}$ space and the dashed curve is for 50% coverage of δ_{cp} values.
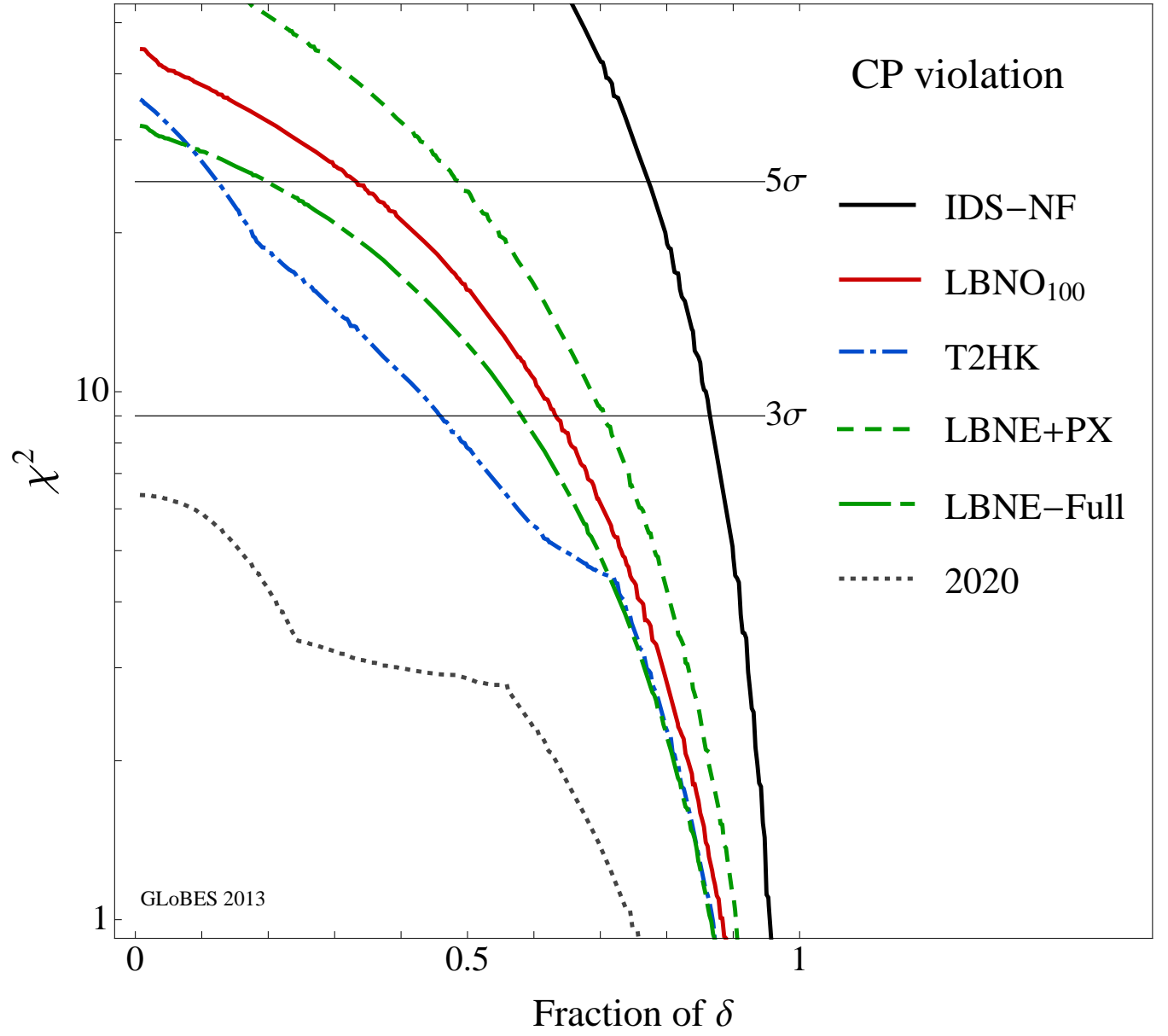
Figure 11: Comparison of the sensitivity to CP violation for different experimental programs at the conclusion of the proposed program.

Table 5: Summary of proposed projects

Project	Cost range	Exposure	CPV reach (25%, 50%, 75%)	$\sigma(\delta_{cp})(°)$	technical readiness
U.S. Experiments					
NoνA 10 yrs	0	100 MW.kT. yrs	$?\sigma$, $?\sigma$, $?\sigma$	26-75 °	extended running
NoνA + GLADE	~ 200 M	120 MW.kT. yrs	$?\sigma$,$?\sigma$, $?\sigma$	22-62 °	
LBNE 35kT	~ 1 B	250 MW.kT.yrs	5σ, 3.8σ, 2.0σ	13-20 °	CD2
LBNE + PX	??	750 MW.kT.yrs	8σ, 6σ, 3.0σ	6-10 °	CD0 for PX
NF Stage 1 + PX	~ 1 \$B				pre-CD0
NF-IDS	multi \$B				pre-CD0
Other regions					
T2HK	???	4600 MW.kT.yrs	5.7σ, 4σ, 2.5σ	7-14 °	advanced
LBNO	???				R&D phase
ESS	???				pre-pre conceptual

3   Summary and Conclusions

The search for CP violation in the neutrino sector required very large mass (10-100 kiloton-scale) neutrino detectors with excellent e/μ particle identification located at a distance of > 1000 km from a high purity beam neutrino source - *regardless of the experimental approach*. A large mass coupled with a powerful beam and long exposures is essential to accumulate enough neutrino interactions – $\mathcal{O}(1000)$ events – to make precision measurements of the parameters that govern the sub-dominant $\nu_\mu \to \nu_e$ oscillations. The LBNE beam design, baseline at 1300km, and the LAr-TPC neutrino detector technology offers the best sensitivity to CP violation using a conventional neutrino beam.

References

[1] C. Jarlskog, Z. Phys **C29**, 491 (1985)

[2] F. Fogli *et al.* Phys.Rev. **D86**, 013012 (2012)

[3] J. Beringer *et al.* (Particle Data Group), Phys. Rev. D86, 010001 (2012)

[4] MINOS Collaboration (P. Adamson et al.) Phys.Rev.Lett. **108** 191801 (2012)

[5] M. Freund, Phys. Rev. **D64**, 053003 (2001)

[6] Nucl.Phys.Proc.Suppl. **221** 166 (2011)

[7] L. Wolfenstein, Phys. Rev. **D17**, 2369 (1978)

[8] G. Fogli, E. Lisi New J.Phys. **6**, 139 (2004)

[9] Borexino Collaboration (M. Buizza Avanzini *et. al.*) Prog.Part.Nucl.Phys. **66**, 412 (2011)

[10] S. Kopp, AIP Conf. Proc. **773**, 276 (2005).

[11] P. Adamson *et al.* (MINOS Collaboration), Phys. Rev. Lett. **110**, 171801 (2013)

[12]

[13] J. Alonso *et al.* "Expression of Interest for a Novel Search for CP Violation in the Neutrino Sector: DAEδALUS", arXiv:1006.0260

[14] R. J. Abrams *et al.* "Interim Design Report", arXiV 1112.2853

[15] Phys. Rev. D87 003004 (2013)

[16] PM. Sajjad Athar *et al.*, Phys. Lett. **B718**, 1375 (2013)